# Seismic control response of structures using an ATMD with fuzzy logic controller and PSO method

Hashem Shariatmadar[a] and Hessamoddin Meshkat Razavi[*]

*Department of Civil Engineering, Ferdowsi University of Mashhad,
Azadi Square, Mashhad, Islamic Republic of Iran*

**Abstract.** This study focuses on the application of an active tuned mass damper (ATMD) for controlling the seismic response of an 11-story building. The control action is achieved by combination of a fuzzy logic controller (FLC) and Particle Swarm Optimization (PSO) method. FLC is used to handle the uncertain and nonlinear phenomena while PSO is used for optimization of FLC parameters. The FLC system optimized by PSO is called PSFLC. The optimization process of the FLC system has been performed for an 11-story building under the earthquake excitations recommended by International Association of Structural Control (IASC) committee. Minimization of the top floor displacement has been used as the optimization criteria. The results obtained by the PSFLC method are compared with those obtained from ATMD with GFLC system which is proposed by Pourzeynali *et al.* and non-optimum FLC system. Based on the parameters obtained from PSFLC system, a global controller as PSFLCG is introduced. Performance of the designed PSFLCG has been checked for different disturbances of far-field and near-field ground motions. It is found that the ATMD system, driven by FLC with the help of PSO significantly reduces the peak displacement of the example building. The results show that the PSFLCG decreases the peak displacement of the top floor by about 10%-30% more than that of the FLC system. To show the efficiency and superiority of the adopted optimization method (PSO), a comparison is also made between PSO and GA algorithms in terms of success rate and computational processing time. GA is used by Pourzeynali *et al* for optimization of the similar system.

**Keywords:** active tuned mass damper (ATMD); fuzzy logic controller (FLC); particle swarm optimization (PSO) method; PSFLCG; displacement reduction; earthquake excitations

## 1. Introduction

Excessive vibrations of structures cause human discomfort and sometimes endanger structural safety. Controlling the peak response of a building subjected to dynamic loads such as earthquakes and winds forces has been a popular area of research for many structural engineers in recent years. In the last four decades, passive and active structural control devices have been developed to suppress the structural vibration. Among them, tuned mass damper (TMD) has attracted the attention of many researchers in the field of passive control devices (Warburton 1982, Villaverde

---

*Corresponding author, Ph.D. Student, E-mail: hessam_meshkat@yahoo.com
[a]Associated Professor, E-mail: Shariatmadar@um.ac.ir

1985, Villaverde and Koyama 1993, Sadek *et al*. 1997, Hadi and Arfiadi 1998, Gattulli *et al*. 2004, Marano *et al*. 2008, Leung and Zhang 2009, Marano *et al*. 2010, Bekdaş and Nigdeli 2011, Lu *et al*. 2012, Tributsch and Adam 2012, Nigdeli and Bekdas 2013, Farshidianfar and Soheili 2013a, b, Matta 2011, Matta 2013). Studies on the performance of TMD shows that a TMD acts well when the frequency of mass damper is coincided with the frequency of loading. The performance of a TMD may decrease when the structure is subjected to earthquake with high-frequency content or when off-optimum parameters are allocated for TMD (i.e., the tuning frequency and the damping ratio). In order to increase the effectiveness of a TMD system, an active control force can be inserted between the structure and TMD (Yao 1972). This new scheme is called active tuned mass damper (ATMD). The ability of the new device mainly relies on the natural motion of mass while; the active control force increases the robustness of TMD. Researchers have also developed a new class of TMD which is called smart or semi-active tuned mass damper (STMD). Nagarajaiah and Jung (2014) have recently presented a journal paper that reported the recent STMD implementations in tall buildings and bridges. STMD system is similar to a TMD system with either variable stiffness and/or variable damping. The response reduction of STMD is comparable to an ATMD, but with the less required magnitude of active control force. STMD has been investigated by many researchers as (Setareh 2001, Varadarajan and Nagarajaiah 2004, Nagarajaiah and Sonmez 2007, Woo *et al*. 2011, Lin *et al*. 2013, Pasala and Nagarajaiah 2014, Contreras *et al*. 2014, Sun *et al*. 2014).

Numerous studies have been performed on the application of ATMD for vibration control of structures. In most of them, modern control techniques are used to obtain the appropriate control force. This active control force is usually calculated within the several constraints. In order to obtain a suitable active force, the researchers have been focused on optimizing the feedback and/or feed-forward gains of the active force in the case of the minimization of the maximum displacement or accelerations of the building under different kinds of excitations (Nishimura *et al*. 1992). The most common optimization algorithms used in these studies are linear quadratic regulator (LQR) (Chang and Soong 1980), pole assignment control method (Abdel-Rohman 1984), $H_2$ and $H_\infty$ (Palazzo and Petti 1999, Park *et al*. 2009), linear quadratic Gaussian (LQG) (Samali *et al*. 2004, Chen *et al*. 2011), sliding mode control (Guclu and Sertbas 2005) and bang-bang control (Collins *et al*. 2006). Recently, Jang *et al*. (2014) used an active mass damper (AMD) system with the time delay control (TDC) algorithm, for effectively suppressing the excessive vibration of a building under wind loading. Xu *et al*. (2014) designed a pair of active mass driver (AMD) systems which has been installed on the top of the Canton Tower for suppressing the wind-induced vibrations. The AMD system driven by permanent magnet synchronous linear motors are adopted. All the outlined studies used the methods that are usually gradient-based and need substantial mathematical calculations.

In other studies, novel algorithm such as fuzzy logic controller (FLC) is used to apply the appropriate control force to ATMD (Samali and Al-Dawod 2003, Samali *et al*. 2004, Wang and Lin 2007, Shariatmadar *et al*. 2014). The fuzzy controller can be easily implemented by using human experience. The advantage of the fuzzy approach is its inherent robustness and its ability to handle the nonlinear and uncertain phenomena existed in structural elements and also in earthquake excitations. The fuzzy approach does not have a mathematical model; instead it is based on human experience. In addition, for implementation of the fuzzy system, limited number of measured structural responses is needed.

Battaini *et al* (1998) studied the potential of the fuzzy logic controller in an AMD for a 3-story benchmark building under earthquake ground acceleration. They firstly presented the application

of fuzzy controller in an AMD. Samali *et al*. (2004) evaluated the efficiency of an ATMD for wind vibration control of a 76-story benchmark building, where the control action is achieved by fuzzy logic controller. They checked the robustness of the controller by reanalyzing the building with different initial stiffnesses. The results also showed that the FLC system outperform LQG controller. In another study, Al-Dawod *et al*. (2006) demonstrated the performance of the FLC system by constructing a scaled 5-story benchmark model with an ATMD and vibrated it on a shake table. They compared the results obtained by FLC with that of the LQR. The results showed that the FLC perform similar to LQR controller in terms of response reduction and amount of the required active control force. In both studies of Samali *et al*. (2004), Al-Dawod *et al*. (2006), triangular membership functions have been selected for input and output variables. Guclu and Yazici (2008) investigated the efficiency of the fuzzy logic controller in an ATMD placed on the fiftieth floor of a 15-story building. They evaluated the performance of FLC under the Kocaeli and Kobe earthquakes. A comparison is also made between Proportional Derivative (PD) controller and FLC system. The results show that FLC has a better performance than PD controller in term of amplitude response reduction. Aly (2014) designed an ATMD for reducing the responses of high-rise buildings under multidirectional wind loads. The active control force is carried out through the LQG and fuzzy logic controllers. They found that the fuzzy logic controller may be more robust than the LQG controller. Shariatmadar *et al*. (2014) examined the application of interval valued fuzzy logic controller (IVFLC) in an ATMD for decreasing the structural response of an 11-story building under the IASC earthquake excitations.

In all the outlined studies, the membership functions have been usually selected by a trial and error approach for the purpose of achieving a good control performance. This way obviously does not result in an optimum solution. Therefore, some researchers were inclined to the applicability of optimization methods for improving the performance of FLC system. In few investigations, Genetic Algorithm (GA) is used as the optimizer tool for designing an optimized FLC system (Ahlawat and Ramaswamy 2002, Pourzeynali *et al*. 2007). Ahlawat and Ramaswamy (2002) applied an ATMD driven by FLC for controlling wind-induced vibration of a 76-story benchmark problem. They used GA for optimization of FLC and ATMD parameters. The input and output variables had Gaussian membership functions. They also showed that using acceleration and velocity as the feedback parameters leads to the satisfied results. Pourzeynali *et al*. (2007) proposed a combined application of fuzzy logic controller (FLC) and genetic algorithm (GA). The FLC has been designed to estimate the active control force, while GA has been utilized to optimize the damper characteristics and membership function parameters. The combined controller is applied to an 11-story building. The results of building's analysis showed that the required active control force in FLC is more than that needed in LQR system, while the response reduction with FLC is more than those obtained by LQR. These studies (Ahlawat and Ramaswamy 2002, Pourzeynali *et al*. 2007) show that the integration of the fuzzy logic controller and GA provide the better performance of the controlled structure with ATMD.

In comparison with GA, PSO algorithm was proposed by Kennedy and Eberhart (1995). This algorithm has some appealing features such as easy application, fast convergence rate and few required computational processing times. PSO was originated from the social behavior of birds' flock migrating to reach to an unknown destination. From then till now, PSO has been successfully applied for optimization of many types of engineering problems (Leung *et al*. 2008, Leung and Zhang 2009, Chen *et al*. 2009, Tang *et al*. 2013).

In this study, a combination of particle swarm optimization (PSO) method and fuzzy logic controller (FLC) has been presented. FLC is used to activate an ATMD installed on the top floor of

an 11-story building and PSO is utilized to get the optimum parameters of FLC system. Minimization of the maximum displacement of the top floor of the example building is regarded as the optimization criteria. The optimization process has been performed for each of the IASC earthquakes excitation. Based on the obtained parameters, the global coefficients for FLC system are introduced for engineering designers. The new control scheme is called PSFLCG. The robustness of the PSFLCG is checked for different earthquake excitations including both far-field and near-field records. The response of the structure controlled with ATMD through PSFLCG is compared with the uncontrolled structure and structure with ATMD through non-optimum FLC system. The results show that the PSFLCG decreases the peak displacement of the top floor by about 10%-30% more than that of the FLC while the required control forces in both systems are approximately the same. Finally, a comparison is made between PSO and GA (GA has been used as the optimizer tool for FLC systems). The superiority of PSO to GA has been proven in terms of success rate, computational processing times and solution quality.

## 2. Structural model

The model used in this study is an 11-story building located in Islamic Republic of Iran (Pourzeynali *et al*. 2007) (See Fig. 1). Since the floors' levels have been assumed entirely rigid, the structure has 11 degrees of freedom in horizontal direction. The properties (mass and stiffness of floors) of the building are provided in Table 1. An ATMD is placed on the top floor of the building for mitigation of the building induced-vibration. An active control force is implemented by an actuator and it is estimated through the fuzzy logic approach.

The equation of motion for a multi-degree-of-freedom system subjected to earthquake ground motion is presented as follows

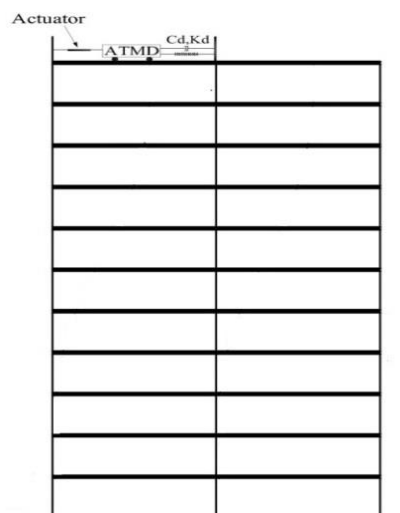$$[M]\{\ddot{y}\} + [C]\{\dot{y}\} + [K]\{y\} = [M]\{E\}\ddot{x}_g + [E_f]F \tag{1}$$



Fig. 1 11-storey shear building with ATMD

Table 1 Parameters of the 11-story building

| Story | Mass (kg) | Stiffness (N/m) |
|:-----:|:---------:|:---------------:|
| 1 | 215370 | 4.68E+08 |
| 2 | 201750 | 4.76E+08 |
| 3 | 201750 | 4.68E+08 |
| 4 | 200930 | 4.50E+08 |
| 5 | 200930 | 4.50E+08 |
| 6 | 200930 | 4.50E+08 |
| 7 | 203180 | 4.50E+08 |
| 8 | 202910 | 4.37E+08 |
| 9 | 202910 | 4.37E+08 |
| 10 | 176100 | 4.37E+08 |
| 11 | 66230 | 3.12E+08 |

$\{\ddot{y}\}$, $\{\dot{y}\}$ and $\{y\}$ are the acceleration, velocity and displacement floors' vectors. $E$ is the influence vector which represents a column of ones. $E_f$ indicates the location of the control force. $[M]$, $[C]$ and $[K]$ are the mass, damping and stiffness matrices of the combined structure and ATMD. F is the active control force. $\ddot{x}_g$ is the earthquake excitations. The International Association of Structural Control (IASC) has identified four earthquake records to be used to check the performance of any control system for seismic applications. These earthquake records are two far-field (El-Centro 1940, Hachinohe 1968) and two near-field (Northridge 1994, Kobe 1995). The original absolute peak ground acceleration (PGA) of the El-Centro, Hachinohe, Kobe and Northridge earthquakes are 0.3417 g, 0.225 g, 0.8178 g and 0.8267 g, respectively. El-Centro and Hachinohe with their original intensity, Northridge with 30% of its original intensity and Kobe with 40% of its original intensity are used in this study (Samali and Al-Dawod 2003). Kobe and Northridge earthquakes cause nonlinear action in structural elements due to their high peak ground accelerations (PGAs). Nonlinearity is appeared in terms of great displacements and formation of plastic hinges. The reduction in near-field PGAs is applied to provide linear behavior for the structural elements.

Since masses are assumed entirely lumped at the floors' level and degrees of freedom are only considered in the horizontal direction, the mass matrix has an orthogonal form. A shearing stiffness matrix is provided as the floors' slabs are assumed rigid. The structural damping matrix is calculated according to the Rayleigh's method. Taking the structural damping ratio as the 5% of the critical damping value for the first two modes, the damping matrix can be calculated as the following procedure

$$[C] = a_1[M] + a_2[K] \tag{2}$$

$$a_1 = \xi \frac{2w_1 w_2}{w_1 + w_2}, \quad a_2 = \xi \frac{2}{w_1 + w_2} \tag{3}$$

The coefficients $a_1$ and $a_2$ are obtained from Eq. (3). $w_1$ and $w_2$ are the first and second natural frequencies of the uncontrolled structure and calculated as 6.5727 and 19.355 rad/s, respectively. The ATMD system consists of a lumped mass of 3% of the total mass of the building (Pourzeynali *et al.* 2007). The ATMD is tuned to the fundamental frequency of the structure (first mode) and its damping ratio is taken as 7% of its critical value (Pourzeynali *et al.* 2007).

For a fast and easy analysis, the equation of motion (Eq. (1) is converted into state space equation as

$$\{\dot{x}\} = [A]\{x\} + \{B_f\}F + \{B_g\}\ddot{x}_g \tag{3}$$

Where

$$x = \begin{Bmatrix} y \\ \dot{y} \end{Bmatrix}, \quad B_f = \begin{Bmatrix} 0 \\ M^{-1}.E_f \end{Bmatrix}, \quad B_g = \begin{Bmatrix} 0 \\ -E \end{Bmatrix}$$

$$A = \begin{bmatrix} 0 & I \\ -M^{-1}.K & -M^{-1}.C \end{bmatrix}$$

*I* is an identity matrix.

## 3. Fuzzy Logic Controller (FLC)

The fuzzy logic theory was firstly introduced by Zadeh (1975). A fuzzy system employs linguistic phrases to execute an appropriate control force. The most important difference between fuzzy systems and traditional mathematically-based optimization methods is that the fuzzy theory gives a degree between (0, 1) to an object while traditional methods specifies 0 or 1 degree to an object. So doing, the fuzzy theory can cover uncertainty and nonlinearity. Uncertainty can arise in different ways such as induced-vibration and also by the sensors measurement. Nonlinear behaviours are observed in two ways: the large displacement (*P*-delta effect) and the failure of structural elements due to yielding. In this study, uncertainty is considered by taking various types of earthquake excitations and nonlinearity is ignored.

The fuzzy inference system is based on If-Then rules. An If-Then rule consists of two parts: antecedent and consequent. For example, a rule can be written as follows:

If $x_1 = A_1$ and $x_2 = A_2$ … and $x_n = A_n$ Then $y = B$

Where $x_i$ ($i = 1, …, n$), and y are the input and output data, respectively. $A_i$ and $B$ are the fuzzy variables. To achieve a desired control level, a collection of If-Then rules are needed. These rules are usually constructed by experts and used to organize the fuzzy associated memory (FAM). A fuzzy logic controller is composed of four main parts as graphically illustrated in Fig. 2.

-Fuzzification

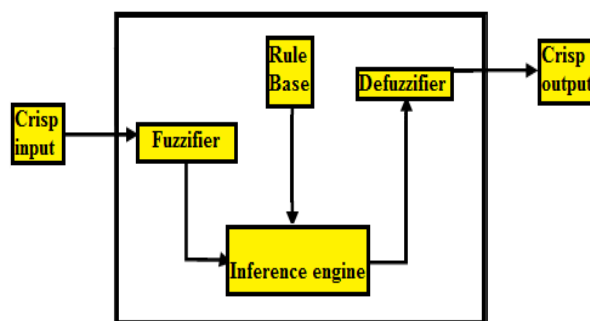In this part, the measured variables in the form of crisp value must be converted into fuzzy sets.



Fig. 2 Structure of a fuzzy logic system

Doing this, the input data in the form of fuzzy sets are got ready to enter into the fuzzy reasoning machine.
-Fuzzy Rule Base

Fuzzy rule base consists of a set of If-Then rules. The rules have been established by the knowledge of different experts. These rules are gathered together to provide a desirable control level.
-Inference Engine

It is the brain of a fuzzy system in the sense that all the fuzzy rule bases are combined together and represent a mapping from fuzzy input set into a fuzzy output set. So doing, the output data are transformed in the form of fuzzy sets. The most commonly used fuzzy inference engine in FLC systems, which is also used in this study, is the Mamdani inference engine.
-Defuzzification

The output data (the control force) in the form of fuzzy set should be converted into a crisp value. In this study, center of average (COA) is used as defuzzification method to obtain the output crisp data.

## 4. Fuzzy control design

A fuzzy control system is preferred when engineers are challenged with the design of a control system for complex structures. In this type of structures, it is very difficult to use traditional controllers like LQG, LQR, $H_2$, $H_\infty$ and…, where the accuracy of controllers dramatically depends on the precise and accurate dynamic model of the structure.

FLC, as an intelligent controller, can be easily designed and implemented in a wide range of structures. A FLC system is free from the mathematical model. Similar to traditional optimization methods, FLC usually handles the system through a close-loop or an open-loop manner.

Since the largest response of the building is occurred at the top floor, the displacement and velocity of the eleventh story are regarded as the feedback parameters. It is notable that LQR -as the most common control algorithm- requires 22 input variables (displacement and velocity of all floors) for a full state feedback implementation in the same structure. The main purpose of using these two variables is to show the ability of fuzzy controller in which only little initial information is required.

The controller is designed with two input variables, each having 3 triangular membership functions (Fig. 3) and one output variable with 7 triangular membership functions (Fig. 4). All the membership functions have been defined on the common interval [-1, 1]. In the non-optimum FLC system, *a*, *b*, *c*, *d*, *e*, *f* are chosen as 0, 1, -1, 0, 1 and -1, respectively. The input subsets are N₌ Negative, Z₌ Zero, P₌ Positive and the output subset are NB₌ Negative Big, NM₌ Negative Medium, NS₌ Negative Small, Z₌ Zero, PS₌ Positive Small, PM₌ Positive Medium, PB₌ Positive Big

These feedback components express the performance of the fuzzy system. For example, if the displacement is zero and velocity is not zero, control force with small intensity should be applied to return the structure to the neutral position. On the other hand, if displacement and velocity are of the same sign, structure is getting far from the equilibrium position, therefore; the control action with high intensity is needed for restoring the structure to its primary position. At the intermediate state, when displacement is negative or positive with approximately zero velocity, the relatively medium control force is needed.  At last, if displacement and velocity are of the apposite sign, the
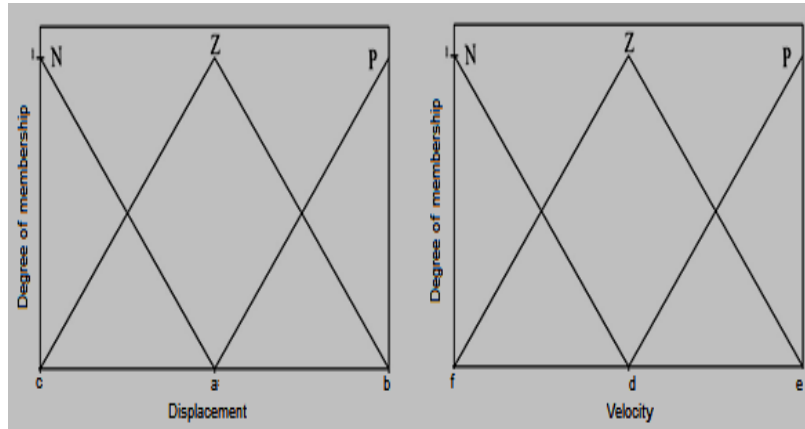
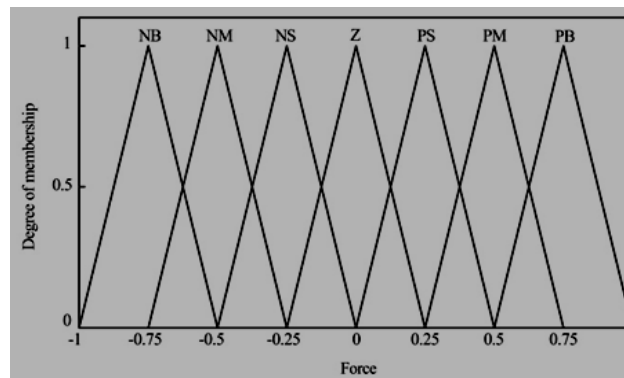Fig. 3 Membership functions for input variables (displacement and velocity)



Fig. 4 Membership functions for output variable (control force)

structure is returning toward the neutral position due to its restoring force, hence a small control force should be applied. Therefore, it is observed that a combination of velocity and displacement feedback provides a perfect decision on making the control action.

In most of studies, experts define the type and characteristic of membership functions (MFs). Due to their various aspects of points about the magnitude of input variables in different earthquake excitations, membership functions can be presented in different forms (triangular, trapezoidal, Gaussian and bell shape). Among highly applied MFs, the triangular membership functions are formed of straight lines. This type of membership functions are simple to implement and fast for computation and used in many studies similar to our work (Al-Dawod *et al*. 2001, Samali and Al-Dawod 2003, Samali *et al*. 2004, Shariatmadar *et al*. 2014). This way may not result in an optimum solution. In few investigations (Ahlawat and Ramaswamy 2002, Pourzeynali *et al*. 2007), GA has been used as an optimizer tool for initial design of the FLC system. In this study, particle swarm optimization (PSO) method is used to optimize the fuzzy parameters. In this paper, the significance use of the optimized input membership function and comparison with that of the off-optimum ones has been considered. The optimization process has been only performed for input membership functions while the output membership functions are not in the optimized

form. Hence, the centers of membership functions of the input variables (*a*, *b*, *c*, *d*, *e* and *f*) as shown in Fig. 3, have been selected as the optimization factors.

## 5. Particle swarm optimization

The difficulties associated with conventional optimization methods have contributed to the rapid development of metaheurestic optimization algorithms. James Kennedy (social psychologist) and Russel Eberhart (electrical engineer) proposed an evolutionary technique in 1995 named as particle swarm optimization (PSO) method. PSO is inspired by the behavior of swarms in the nature such as birds, fish, and … moving to reach the unknown destination. PSO method like all the metaheurestic algorithms, find the optimum solution of a problem with lots of iterations. In PSO, each solution is a bird in the flock referred to as a particle. This algorithm uses a collection of flying birds (different solutions) that communicate together as they fly. Each bird flies in a specific direction and identify the birds that is in the best location (best solution). Each bird speeds towards the best bird using a velocity that depends on its current position. Then, each bird investigates the search space from its new local position. The process repeats until the flock (solutions) reaches a desired destination (optimum solution). The most important advantage of PSO method is that the birds use both their own experience and other birds' experience to accede the desired destination. The procedure of PSO can be summarized as the following:

Step1: The process is initialized with generating population of *N* particles (*N* Solutions) with random positions and velocities. The *i*th particle is represented by its position as a point in a d-dimensional space. *d* is the number of variables that should be optimized (*d*=6).

Step 2: For each particle, the objective function -*f*(*x*)- is evaluated. In this study, the minimization of the peak displacement value of the top floor of an 11-story building due to earthquake excitation is considered as the objective function. Each particle has a current position $X_i=(x_{i1},...,x_{id})$ and velocity $V_i=(v_{i1},...,v_{id})$. The *i*th particle has its own best position, $pBest_i=(p_{i1},...,p_{id})$ that reaches in the previous cycles. In this step the position of the best particles ($gBest_i$) is calculated as it has the best (minimum) value of the objective function *f*(*x*) among all the particles.

Step 3: The new position and velocity of each particle are updated to catch up with the best particle and given by Eqs. (4) and (5)

$$\text{New } V_i = W \times \text{Current } V_i + C_1 \times \text{Rand}_1(\,) \times (pBest_i\text{-}X_i) + C_2 \times \text{Rand}_2(\,) \times (gBest_i\text{-}X_i) \qquad (4)$$

$$\text{New position } X_i = \text{Current position } X_i + \text{New } V_i \qquad (5)$$

Where $C_1$ and $C_2$ are the two positive constants named as acceleration coefficient. W is the inertia factor. It plays the role of balancing between the global search and local search and was proposed to decrease linearly from 1.4 to 0.5. $\text{Rand}_1$ and $\text{Rand}_2$ are two independent random functions in the range of [0, 1]. $V_i$ is restricted between -$V_{max}$ and $V_{max}$.

Step4: The objective function is again calculated for the new particles. Once the new position of a particle is calculated, the particle flies toward it.

Step 5: The process is continued for B times. B is the number of iterations. After that, the global best position and its optimized parameters are obtained. Now, the procedure is come to an end.

The parameters of PSO used in this study are given as follows: *B*=100, *N*=20, $C_1$=$C_2$=2, *W*=1, $V_{max}$=2
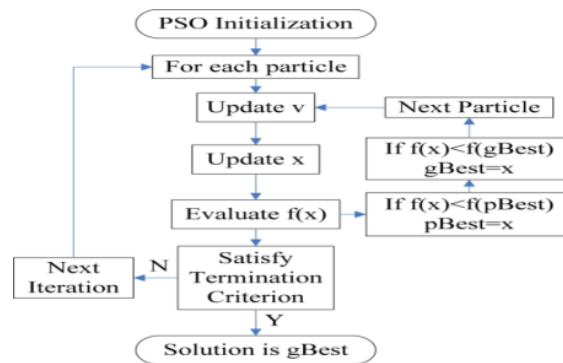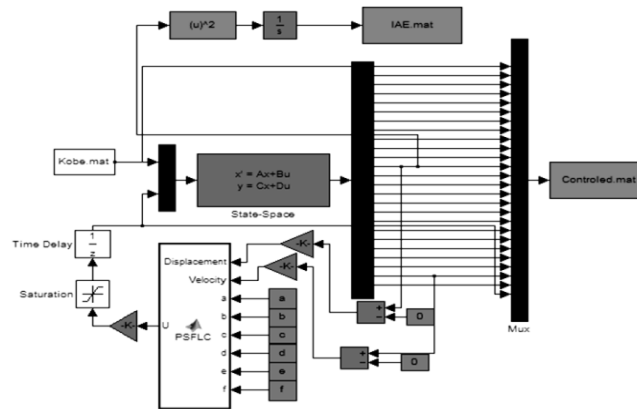
Fig. 5 Flowchart of PSO algorithm



Fig. 6 Simulink model for the 11-story building with PSFLC

The flowchart depicting the PSO algorithm is shown in Fig. 5

## 6. Numerical study

In order to investigate the optimum parameters of the FLC system, an 11-story shear building is considered. The example building is a reduced form of a realistic designed building. This 11-story building is located in the city of Rasht, Iran. For taking a fast and general analysis the building is transformed into a 2-dimensional shear building. The adopted control scheme consists of an active tuned mass damper (ATMD) placed on the top floor of the building. The control action is achieved by the fuzzy logic system. The PSO algorithm is used to find the optimum centers' value of input membership function in which the maximum displacement of the top floor is minimized. The simulation analysis has been performed by Matlab Software (See Fig. 6) for each of the IASC earthquake excitations, separately. The optimized parameters are provided in Table 2. The optimized FLC system is called PSFLC.

Table 3 shows the peak displacement of the top floor for the uncontrolled structure and controlled structure with ATMD through FLC, PSFLC and GFLC systems for IASC earthquake

Table 2 Optimized membership function parameters

| Earthquake excitation | | | Optimized Parameters | | | | | | | | | | |
|---|---|---|---|---|---|---|---|---|---|---|---|---|---|
| | | | $a$ | | $b$ | | $c$ | | $d$ | | $e$ | | $f$ |
| 1 | Hachinohe | $a_1$ | -1 | $b_1$ | 0.2020 | $c_1$ | -0.6078 | $d_1$ | 0.1981 | $e_1$ | 1 | $f_1$ | -0.9675 |
| 2 | El-Centro | $a_2$ | -1 | $b_2$ | 0.8396 | $c_2$ | -0.2665 | $d_2$ | 0.1183 | $e_2$ | 0.7282 | $f_2$ | -0.4027 |
| 3 | Kobe | $a_3$ | 0 | $b_3$ | 0.5431 | $c_3$ | 0 | $d_3$ | -0.1265 | $e_3$ | 0.6973 | $f_3$ | -1 |
| 4 | Northridge | $a_4$ | 0.2461 | $b_4$ | 1 | $c_4$ | -1 | $d_4$ | 0.2532 | $e_4$ | 1 | $f_4$ | -1 |

Table 3 Peak top floor displacement for different control systems under the IASC earthquake excitation

| Earthquake Excitation | Peak displacement of top floor (m) | | | | Response reduction (%) | | |
|---|---|---|---|---|---|---|---|
| | Uncontrolled Response | Controlled Response | | | | | |
| | | FLC | PSFLC | GFLC | | | |
| Hachinohe | 0.109 | 0.0668 | 0.0308 | 0.0572 | 38.5 | 71.6 | 47.5 |
| El-Centro | 0.145 | 0.0843 | 0.0595 | 0.0520 | 41.7 | 58.9 | 64.1 |
| Kobe | 0.192 | 0.1116 | 0.0741 | 0.148 | 41.8 | 61.3 | 22.9 |
| Northridge | 0.071 | 0.0608 | 0.0602 | 0.051 | 14.8 | 15.7 | 28.1 |

excitations. GFLC system has been proposed by Pourzeynali *et al*. (2007) in which the fuzzy system has been optimized with GA for the presented structure and the same earthquake excitations. They have used 5 trapezoidal membership functions for 2 input variables (displacement and velocity of the top floor) and 7 triangular membership functions for output variable (control force). They have assumed the same optimized membership functions for both displacement and velocity variables. The output membership function and the weighting coefficient of the fuzzy associative memory (FAM) rules have been also optimized. The percentage reduction in maximum displacement of the top floor with respect to the response of the uncontrolled building for different control systems are provided in Table 3.

From Table 3, it is understood that the PSFLC decreases the peak response of the top floor more than those obtained by FLC system. The reduction in peak displacement response of the top floor for PSFLC is 33% and 17% more than the FLC for Hachinohe and El-Centro earthquake excitations, respectively. For Kobe earthquake excitations, the relevant reduction for PSFLC is 20% more than that obtained by the FLC system. The corresponding reduction for FLC and PSFLC are approximately equal for Northridge earthquake. The simulation results show that the FLC system with non-optimum parameters cannot reduce the peak displacement of the top floor more than that of the PSFLC system. The results also show that the proposed controller (PSFLC) reduces the peak displacement of the 11-story building more than those obtained by GFLC method for Hachinohe and Kobe earthquakes by about 25% and 40%. Furthermore, it is understood that both PSFLC and GFLC controllers have approximately the same performance for El-Centro earthquake excitation. However, GFLC outperform PSFLC in Northridge earthquake. It reduces the peak displacement of the top floor by about 12% more than that of the PSFLC approach.

In order to obtain global coefficients, PSO method is utilized again. The coefficients $a_g$, $b_g$, $c_g$, $d_g$, $e_g$ and, $f_g$ are considered as design variables. The objective is to minimize the Root Mean Square (RMS) of errors for each of the global parameter in the case of using the IASC earthquake excitations. The global coefficients are computed as follows

$$E(a_g) = [\frac{1}{N}\sum_{i=1}^{N}(a_g - a_i)]^{1/2} \qquad (6)$$

In the above formula, $N$ is the number of earthquake excitation, $a_i$ is the optimum parameter related to the $i$th earthquake and $a_g$ is the global coefficient. In the same way, this formulation is applied for obtaining the other global parameters ($b_g$, $c_g$, $d_g$, $e_g$ and, $f_g$ ). Finally, the global values for centers of input membership functions are obtained as follows:

$a_g$= -0.4385, $b_g$= 0.6462, $c_g$= -0.4686, $d_g$= 0.1108, $e_g$= 0.8564 and $f_g$= -0.8425

The optimized FLC system with global coefficient is called PSFLCG. Now, the robustness of this new control scheme has to be checked.


## 7. Robustness of PSFLC

In order to check the robustness of the proposed controller, the PSFLCG outlined previously is employed to the ATMD of example building. The simulation analysis of the 11-story building with an ATMD system and PSFLCG controller is conducted using 2 far-field and 4 near-field earthquake records. The characteristic of the new earthquakes are presented in Table 4. Since structural safety is depended to the maximum displacement of floors, it is taken as the comparative criterion for checking the ability of PSFLCG system versus FLC system.

The peak displacement of floors associated with the response reduction for different control systems along with the uncontrolled response subjected to various earthquake excitations are presented in Table 5. As can be observed from the results in Table 5, the FLC reduces the peak displacement of the floors of model by an average about 24% and 34% for Kern-County and Chi-Chi earthquake records, respectively. When using PSFLCG as the control system, the corresponding reductions are about 41% and 54% for Kern-County and Chi-Chi earthquake records, respectively. Furthermore, the PSFLCG reduces the peak displacement of the top floor by about 35% and 17% more than that of the FLC system for the same earthquake excitations, respectively. This result shows that PSFLCG system outperform FLC in the term of response reduction for far-field earthquake excitations.

Most of control system cannot extremely decrease the response of the building in pulse-like earthquake excitations. In this study, 4 near-fields earthquakes are used to check the performance of the PSFLCG system. The PSFLCG reduces the peak displacement of floors by an average of about 48%, 36%, 26%, and 28%, for Coalinga, Landers, Bam and Nahanni earthquake records, while the corresponding reductions for the FLC system are about 43% and 29%, 22% and 4% for the same earthquakes, respectively. It is noteworthy that PSFLCG reduces the peak displacement of the top floor by about 11%, 10%, 5% and 27% more than those obtained by the FLC system for the near-field earthquake excitations as previously mentioned, respectively. The simulation results also show the ability of the proposed controller (PSFLCG) to reduce the peak displacement of the top floor of model for Coalinga and Landers earthquakes by about 60% and 37%, respectively. Meanwhile, the corresponding reductions are about 29% and 34% for Bam and Nahanni earthquakes, respectively. This result shows that PSFLCG system outperforms FLC in the term of response reduction for near-field earthquake excitations.

Consequently, the results demonstrated that the PSFLCG is robust for different earthquake excitations of both far-field and near-field and perform better than FLC system. The reduction in peak displacement of floors results in smaller size of structural elements.

Table 4 The characteristics of earthquakes

| No. | Earthquake | Type | Date | Station | Time Duration (sec) | PGA(g) |
|-----|-----------|------|------|---------|--------------------|--------|
| 1 | Kern-County | Far-field | 1952/07/21 | 1095 Taft Lincoln School | 54.15 | 0.178 |
| 2 | Chi-Chi | Far-field | 1999/09/20 | CHY101 | 89.95 | 0.353 |
| 3 | Coalinga | Near-field | 1983/07/22 | 1651 Transmitter Hill | 21.75 | 0.84 |
| 4 | Landers | Near-field | 1992/06/28 | 24 Lucerne | 48.12 | 0.785 |
| 5 | Nahanni | Near-field | 1985/12/23 | 6097 Site 1 | 20.55 | 0.97 |
| 6 | Bam | Near-field | 2003/12/26 | NEIC | 58.33 | 0.82 |

Table 5 Peak response of displacement for different control systems under the four earthquake excitations

| Story | Peak Displacement (m) Uncontrolled Response | Controlled Response FLC | Controlled Response PSFLCG | Rresponse Reduction (%) FLC | Rresponse Reduction (%) PSFLCG | Story | Peak Displacement (m) Uncontrolled Response | Controlled Response FLC | Controlled Response PSFLCG | Rresponse Reduction (%) FLC | Rresponse Reduction (%) PSFLCG |
|---|---|---|---|---|---|---|---|---|---|---|---|
| | Kern-County | | | | | | Chi-Chi | | | | |
| 1 | 0.0095 | 0.0068 | 0.0058 | 28.4 | 38.9 | 1 | 0.0235 | 0.0176 | 0.0122 | 25.1 | 48.1 |
| 2 | 0.0186 | 0.0134 | 0.0115 | 28.0 | 38.2 | 2 | 0.0463 | 0.0341 | 0.0237 | 26.3 | 48.8 |
| 3 | 0.027 | 0.0196 | 0.017 | 27.4 | 37.0 | 3 | 0.0679 | 0.0489 | 0.034 | 28.0 | 49.9 |
| 4 | 0.035 | 0.0256 | 0.0223 | 26.9 | 36.3 | 4 | 0.089 | 0.0624 | 0.0432 | 29.9 | 51.5 |
| 5 | 0.0421 | 0.0311 | 0.0268 | 26.1 | 36.3 | 5 | 0.1085 | 0.0739 | 0.0518 | 31.9 | 52.3 |
| 6 | 0.048 | 0.036 | 0.0303 | 25.0 | 36.9 | 6 | 0.1265 | 0.083 | 0.0586 | 34.4 | 53.7 |
| 7 | 0.0534 | 0.0404 | 0.0327 | 24.3 | 38.8 | 7 | 0.1425 | 0.0899 | 0.0633 | 36.9 | 55.6 |
| 8 | 0.0582 | 0.0447 | 0.0342 | 23.2 | 41.2 | 8 | 0.1563 | 0.0946 | 0.0662 | 39.5 | 57.6 |
| 9 | 0.0617 | 0.0484 | 0.0347 | 21.6 | 43.8 | 9 | 0.1665 | 0.0975 | 0.0676 | 41.4 | 59.4 |
| 10 | 0.0636 | 0.0514 | 0.0344 | 19.2 | 45.9 | 10 | 0.1723 | 0.0993 | 0.0687 | 42.4 | 60.1 |
| 11 | 0.0644 | 0.0554 | 0.0331 | 14.0 | 48.6 | 11 | 0.1746 | 0.1013 | 0.0723 | 42.0 | 58.6 |
| | Peak Displacement (m) Uncontrolled Response | Controlled Response FLC | Controlled Response PSFLCG | Rresponse Reduction (%) FLC | Rresponse Reduction (%) PSFLCG | | Peak Displacement (m) Uncontrolled Response | Controlled Response FLC | Controlled Response PSFLCG | Rresponse Reduction (%) FLC | Rresponse Reduction (%) PSFLCG |
| | Coalinga | | | | | | Landers | | | | |
| 1 | 0.03 | 0.0174 | 0.0173 | 42.0 | 42.3 | 1 | 0.0112 | 0.0082 | 0.0076 | 26.8 | 32.1 |
| 2 | 0.0597 | 0.0349 | 0.0341 | 41.5 | 42.9 | 2 | 0.0221 | 0.0153 | 0.0147 | 30.8 | 33.5 |
| 3 | 0.088 | 0.0518 | 0.0499 | 41.1 | 43.3 | 3 | 0.0319 | 0.0222 | 0.0209 | 30.4 | 34.5 |
| 4 | 0.1151 | 0.0682 | 0.0648 | 40.7 | 43.7 | 4 | 0.0406 | 0.0289 | 0.0265 | 28.8 | 34.7 |
| 5 | 0.1393 | 0.0827 | 0.0773 | 40.6 | 44.5 | 5 | 0.0479 | 0.035 | 0.032 | 26.9 | 33.2 |
| 6 | 0.1604 | 0.0947 | 0.0868 | 41.0 | 45.9 | 6 | 0.0563 | 0.0402 | 0.0363 | 28.6 | 35.5 |
| 7 | 0.1784 | 0.1038 | 0.0931 | 41.8 | 47.8 | 7 | 0.0633 | 0.0443 | 0.0392 | 30.0 | 38.1 |
| 8 | 0.1934 | 0.1096 | 0.096 | 43.3 | 50.4 | 8 | 0.0686 | 0.0475 | 0.0407 | 30.8 | 40.7 |
| 9 | 0.2042 | 0.112 | 0.0957 | 45.2 | 53.1 | 9 | 0.072 | 0.0499 | 0.0421 | 30.7 | 41.5 |
| 10 | 0.2103 | 0.1112 | 0.0923 | 47.1 | 56.1 | 10 | 0.0736 | 0.0517 | 0.0445 | 29.8 | 39.5 |
| 11 | 0.2127 | 0.1072 | 0.0848 | 49.6 | 60.1 | 11 | 0.0745 | 0.0536 | 0.0465 | 28.1 | 37.6 |

Table 5 Continued

| Story | Peak Displacement (m) Uncontrolled Response | Controlled Response FLC | Controlled Response PSFLCG | Rresponse Reduction (%) FLC | Rresponse Reduction (%) PSFLCG | Story | Peak Displacement (m) Uncontrolled Response | Controlled Response FLC | Controlled Response PSFLCG | Rresponse Reduction (%) FLC | Rresponse Reduction (%) PSFLCG |
|---|---|---|---|---|---|---|---|---|---|---|---|
| | Bam | | | | | | Nahanni | | | | |
| 1 | 0.04 | 0.0333 | 0.0324 | 16.8 | 19.0 | 1 | 0.0164 | 0.0165 | 0.0131 | -0.6 | 20.1 |
| 2 | 0.0771 | 0.0631 | 0.0615 | 18.2 | 20.2 | 2 | 0.0311 | 0.0322 | 0.0253 | -3.5 | 18.6 |
| 3 | 0.1126 | 0.0891 | 0.0868 | 20.9 | 22.9 | 3 | 0.0451 | 0.0464 | 0.0361 | -2.9 | 20.0 |
| 4 | 0.1484 | 0.1134 | 0.1097 | 23.6 | 26.1 | 4 | 0.0601 | 0.0593 | 0.0455 | 1.3 | 24.3 |
| 5 | 0.1826 | 0.1374 | 0.1313 | 24.8 | 28.1 | 5 | 0.0742 | 0.0702 | 0.0532 | 5.4 | 28.3 |
| 6 | 0.2135 | 0.1604 | 0.1531 | 24.9 | 28.3 | 6 | 0.0864 | 0.0792 | 0.0597 | 8.3 | 30.9 |
| 7 | 0.2403 | 0.1803 | 0.1722 | 25.0 | 28.3 | 7 | 0.0962 | 0.0874 | 0.0655 | 9.1 | 31.9 |
| 8 | 0.2629 | 0.1971 | 0.1883 | 25.0 | 28.4 | 8 | 0.1041 | 0.0949 | 0.0705 | 8.8 | 32.3 |
| 9 | 0.2799 | 0.2101 | 0.20 | 24.9 | 28.5 | 9 | 0.1096 | 0.1006 | 0.0739 | 8.2 | 32.6 |
| 10 | 0.2898 | 0.2187 | 0.2096 | 24.5 | 27.7 | 10 | 0.1128 | 0.1042 | 0.0755 | 7.6 | 33.1 |
| 11 | 0.2937 | 0.2251 | 0.21 | 23.4 | 28.5 | 11 | 0.1141 | 0.1063 | 0.0755 | 6.8 | 33.8 |

Table 6 Maximum required control force

| Earthquake Excitation | Maximum Control Force (kN) FLC | Maximum Control Force (kN) PSFLCG |
|---|---|---|
| Kern-County | 3998 | 3017 |
| Chi-Chi | 1257 | 1288 |
| Landers | 1193 | 1369 |
| Coalinga | 1984 | 2143 |
| Nahanni | 1489 | 1085 |
| Bam | 1382 | 1428 |

Table 6 shows the maximum required control force for the outlined earthquake records. From Table 6, it can be observed that the active control force in PSFLCG system is relatively similar to that of the FLC system except for Kern-County and Nahanni earthquake records.


## 8. Stability of PSFLCG

Since PSFLCG system does not have a mathematical model, the most important concern about this system is its probable instability. The control stability of PSFLCG can be checked through the ability of the controlled system to return to rest condition following oscillation caused by the external disturbance. Here, the stability of the controller has been checked through specifying an extreme initial condition. An initial displacement ($x$=0.2m) is given to the top floor of the example building. Fig. 7 shows the stability of the PSFLCG controller in terms of control force and displacement response. From Fig. 7, it is observed that PSFLCG drive the system to its neutral position after a severe initial excitation. It can be seen that the PSFLCG is stable.
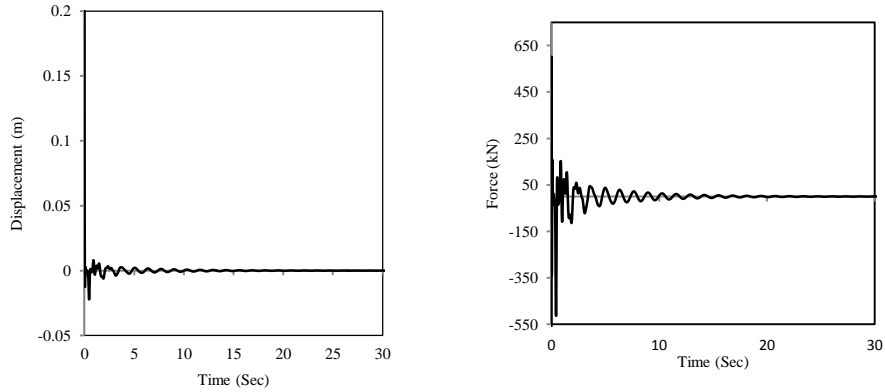
Fig. 7 PSFLC stability test in terms of displacement response and control force

## 9. Comparison between PSO and GA optimization methods

For the sake of comparison between the PSO and GA algorithms, 2 different codes have been written by Matlab 2012 program with a 2.5 GHz core i5 laptop machine. The performance of PSO is compared with GA in terms of convergence speed and computational processing time. In GA optimization process, a new population of chromosomes is formed and replaced with that of the old one, while in PSO process, new birds are not created. The birds evolve their social behavior towards a destination. This is the reason that PSO may perform better than GA.

The convergence speed demonstrates the number of required iterations that an objective function needs to reach its optimum value. The results of the cost function values (maximum top floor displacement) versus the number of iteration are plotted in Fig. 8. It can be seen that PSO is able to reach its optimum value faster than the GA method. Furthermore, PSO gives the lower value of the cost function. It is seen from Fig. 8, that PSO finds the minimum value of the objective function with less than 40 iterations which is 2 times less than the GA approach. The computational processing time to reach the target is also depicted in Fig. 8. It can be found that
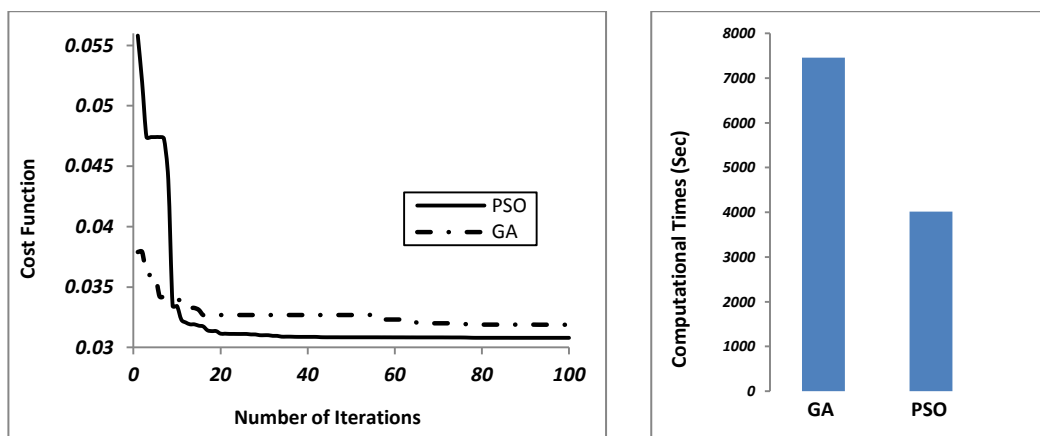


Fig. 8 Convergence rate and computational processing times

the PSO algorithm requires much lesser time to converge. These results show that the PSO algorithm generally outperformed the GA in terms of convergence rate, computational processing time and also cost function value (PSO provides smaller top floor displacement).


## 10. Conclusions

This paper is the first study on the combined application of particle swarm optimization (PSO) method and fuzzy logic controller (FLC) for mitigating the vibration of building under earthquake excitations. Fuzzy membership functions are an important part of a fuzzy system usually defined by the chartered experts. The generalized input membership functions do not result in an optimum solution. In this paper, PSO is utilized to optimize the input fuzzy membership functions. The simulation analysis of an 11-story building with an ATMD was conducted to obtain the optimum parameters of fuzzy system using IASC earthquake excitations. After that, the global coefficients are introduced and the robustness of PSFLCG system has been checked under different ground excitations of both far-field and near-field. The simulation results show that PSFLCG generally outperform the FLC approach. Based on this study some conclusion can be drawn as follows:

• PSFLCG approximately reduces the peak displacement of the top story by about 10%-30% more than that of the FLC.

• PSFLCG reduce the peak displacement of floors by an average of 45% for far-field earthquake excitations and by about 35% for near-field earthquake excitations.

• PSO is a powerful optimizer tool for FLC system in which it finds the optimum solution of the proposed problem faster and with the better success rate and solution quality than that of the GA.


## References

Abdel-Rohman, M. (1984), "Optimal design of active TMD for buildings control", *Build. Environ.*, **19**(3), 191-195.

Ahlawat, A.S. and Ramaswamy, A. (2002), "Multi-objective optimal design of FLC driven hybrid mass damper for seismically excited structures", *Earthq. Eng. Struct. Dyn.*, **31**(7), 1459-1479.

Al-Dawod, M., Samali, B. and Li, J. (2006), "Experimental verification of an active mass driver system on a five-storey model using a fuzzy controller", *Struct. Cont. Hlth. Monit.*, **13**(5), 917-943.

Al-Dawod, M., Samali, B., Naghdy, F. and Kwok, K. (2001), "Active control of along wind response of tall building using a fuzzy controller", *Eng. Struct.*, **23**(11), 1512-1522.

Aly, M.A. (2014), "Vibration control of high-rise buildings for wind: a robust passive and active tuned mass damper", *Smart. Struct. System*, **13**(3), 473-500.

Battaini, M., Casciati, F. and Faravelli, L. (1998), "Fuzzy control of structural vibration. An active mass system driven by a fuzzy controller", *Earthq. Eng. Struct. Dyn.*, **27**(11), 1267-1276.

Bekdaş, G. and Nigdeli, S.M. (2011), "Estimating optimum parameters of tuned mass dampers using harmony search", *Eng. Struct.*, **33**(9), 2716-2723.

Chang, J.C.H. and Soong, T.T. (1980), "Structural control using active tuned mass dampers", *J. Eng. Mech-ASME*, **106**(6), 1091-1098.

Chen, H., Sun, Z. and Sun, L. (2011), "Active mass damper control for cable stayed bridge under construction: an experimental study", *Struct. Eng. Mech.*, **38**(2), 141-156.

Chen, J., Peng, W., Ge, R. and Wei, J. (2009), "Optimal design of composite laminates for minimizing delamination stresses by particle Swarm optimization combined with FEM", *Struct. Eng. Mech.*, **31**(4),

407-421.

Collins, R., Basu, B. and Broderick, B. (2006), "Control strategy using bang–bang and minimax principle for FRF with ATMDs", *Eng. Struct*., **28**(3), 349-356.

Contreras, M.T., Pasala, D.T.R. and Nagarajaiah, S. (2014), "Adaptive length SMA pendulum smart tuned Mass damper performance in the presence of real time primary system stiffness change", *Smart. Struct. System*, **13**(2), 219-233.

Farshidianfar, A. and Soheili, S. (2013a), "ABC optimization of TMD parameters for tall buildings with soil structure interaction", *Interact. Multiscale. Mech*., **6**(4), 339-356.

Farshidianfar, A. and Soheili, S. (2013b), "Ant colony optimization of tuned mass dampers for earthquake oscillations of high-rise structures including soil–structure interaction", *Soil. Dyn. Earthq. Eng*., **51**(0), 14-22.

Gattulli, V., Di Fabio, F. and Luongo, A. (2004), "Nonlinear tuned mass damper for self-excited oscillations", *Wind. Struct*., **7**(4), 251-264.

Guclu, R. and Sertbas, A. (2005), "Evaluation of sliding mode and proportional-integral-derivative controlled structures with an active mass damper", *J. Vib. Control*., **11**(3), 397-406.

Guclu, R. and Yazici, H. (2008), "Vibration control of a structure with ATMD against earthquake using fuzzy logic controllers", *Sound. Vib*., **318**(1-2), 36-49.

Hadi, M.N.S. and Arfiadi, Y. (1998), "Optimum design of absorber for MDOF structures", *J. Struct. Eng-ASCE*, **124**(11), 1272-1280.

Jang, D.D., Jung, H.J. and Moon, Y.J. (2014), "Active mass damper system using time delay control algorithm for building structure with unknown dynamics", *Smart. Struct. System*, **13**(2), 305-318.

Kennedy, J. and Eberhart, R. (1995), "Particle swarm optimization", *Proceedings of the IEEE International Conference on Neural Networks*.

Leung, A.Y.T. and Zhang, H. (2009), "Particle swarm optimization of tuned mass dampers", *Eng. Struct*., **31**(3), 715-728.

Leung, A.Y.T., Zhang, H., Cheng C.C. and Lee, Y.Y. (2008), "Particle swarm optimization of TMD by non-stationary base excitation during earthquake", *Earthq. Eng. Struct. Dyn*., **37**(9), 1223-1246.

Lin, P.Y., Lin, T.K. and Hwang, J.S. (2013), "A semi-active mass damping system for low- and mid-rise buildings", *Earthq. Struct*., **4**(1), 63-84.

Lu, X., Ding, K., Shi, W. and Weng, D. (2012), "Tuned mass dampers for human-induced vibration control of the Expo Culture Centre at the World Expo 2010 in Shanghai, China", *Struct. Eng. Mech*., **43**(5), 607-621.

Marano, G.C., Greco, R. and Chiaia, B. (2010), "A comparison between different optimization criteria for tuned mass dampers design", *Sound. Vib*., **329**(23), 4880-4890.

Marano, G.C., Greco, R. and Palombella, G. (2008), "Stochastic optimum design of linear tuned mass dampers for seismic protection of high towers", *Struct. Eng. Mech*., **29**(6), 603-622.

Matta, E. (2011), "Performance of tuned mass dampers against near-field earthquakes", *Struct. Eng. Mech*., **39**(5), 621-642.

Matta, E. (2013), "Effectiveness of tuned mass dampers against ground motion pulses", *J. Struct. Eng-ASCE*, **139**(2), 188-198.

Nagarajaiah, S. and Jung, H.J. (2014), "Smart tuned mass dampers: recent developments", *Smart. Struct. System*, **13**(2), 173-176.

Nagarajaiah, S. and Sonmez, E. (2007), "Structures with Semiactive Variable Stiffness Single/Multiple Tuned Mass Dampers", *Struct. Eng*., **133**(1), 67-77.

Nigdeli, S.M. and Bekdas, G. (2013), "Optimum tuned mass damper design for preventing brittle fracture of RC buildings", *Smart. Struct. System*, **12**(2), 137-155.

Nishimura, I., Kobori,T., Sakamoto, M., Koshika, N., Sasaki, K. and Ohrui, S. (1992), "Active tuned mass damper", *Smart. Material. Struct*., **1**(4), 306.

Palazzo, B. and Petti, L. (1999), "Optimal structural control in the frequency domain: Control in norm $H_2$ and $H_\infty$", *J. Struct. Cont*., **6**(2), 205-221.

Park, S.J., Lee, J., Jung, H.J., Jang, D.D. and Kim, S.D. (2009), "Numerical and experimental investigation

of control performance of active Mass damper system to high-rise building in use", *Wind. Struct.*, **12**(4), 313-332.

Pasala, D.T.R. and Nagarajaiah, S. (2014), "Adaptive-length pendulum smart tuned Mass damper using shape-memory-alloy wire for tuning period in real time", *Smart. Struct. System*, **13**(2), 203-217.

Pourzeynali, S., Lavasani, H.H. and Modarayi, A.H. (2007), "Active control of high rise building structures using fuzzy logic and genetic algorithms", *Eng. Struct.*, **29**(3), 346-357.

Sadek, F., Mohraz, B., Taylor, A.W. and Chung, R.M. (1997), "A method of estimating the parameters of tuned mass dampers for seismic applications", *Earthq. Eng. Struct. Dyn.*, **26**(6), 617-635.

Samali, B. and Al-Dawod, M. (2003), "Performance of a five-storey benchmark model using an active tuned mass damper and a fuzzy controller", *Eng. Struct.*, **25**(13), 1597-1610.

Samali, B., Al-Dawod, M., Kwok , K. and Naghdy, F. (2004), "Active control of cross wind response of 76-Story tall building using a fuzzy controller", *J. Eng. Mech- ASME*, **130**(4), 492-498.

Setareh, M. (2001), "Use of semi-active Mass dampers for vibration control of force-excited structures. " *Struct. Eng. Mech.*, **11**(4), 341-356.

Shariatmadar, H., Golnargesi, S. and Akbarzadeh T.M.R. (2014), "Vibration control of buildings using ATMD against earthquake excitations through interval type-2 fuzzy logic controller", *Asian. J. Civil. Eng-Bhrc*, **15**(3), 321-338.

Sun, C., Nagarajaiah, S. and Dick, A.J. (2014), "Family of smart tuned mass dampers with variable frequency under harmonic excitations and ground motions: closed-form evaluation", *Smart. Struct. System*, **13**(2), 319-341.

Tang, H., Zhang, W., Xie, L. and Xue, S. (2013), "Multi-stage approach for structural damage identification using Particle Swarm optimization", *Smart. Struct. System*, **11**(1), 319-341.

Tributsch, A. and Adam, C. (2012), "Evaluation and analytical approximation of Tuned Mass Damper performance in an earthquake environment ", *Smart. Struct. System*, **10**(2), 69-86.

Varadarajan, N. and Nagarajaiah, S. (2004), "Wind response control of building with variable stiffness tuned mass damper using empirical mode decomposition/Hilbert transform", *J. Eng. Mech- ASME*, **130**(4), 451-458.

Villaverde, R. (1985), "Reduction seismic response with heavily-damped vibration absorbers", *Earthq. Eng. Struct. Dyn.*, **13**(1), 33-42.

Villaverde, R. and Koyama, L.A. (1993), "Damped resonant appendages to increase inherent damping in buildings", *Earthq. Eng. Struct. Dyn.*, **22**(6), 491-507.

Wang, A.P. and Lin, Y.H. (2007), "Vibration control of a tall building subjected to earthquake excitation", *Sound. Vib.*, **299**(4-5), 757-773.

Warburton, G.B. (1982), "Optimum absorber parameters for various combinations of response and excitation parameters", *Earthq. Eng. Struct. Dyn.*, **10**(3), 381-401.

Woo, S.S., Lee, S.H. and Chung, L. (2011), "Seismic response control of elastic and inelastic structures by using passive and semi-active tuned mass dampers", *Smart. Struct. System*, **8**(3), 239-252.

Xu, H.b., Zhang, C.w., Li, H., Ping, T., Ou, J.p. and Zhou, F.l. (2014), "Active mass driver control system for suppressing wind-induced vibration of the Canton Tower", *Smart. Struct. System*, **13**(2), 281-303.

Yao, J.T.P. (1972), "Concept of Structural Control", *J. Struct. Div.*, **98**(7), 1567-1574.

Zadeh, L.A. (1975), "The concept of a linguistic variable and its application to approximate reasoning-I", *Inform. Sci.*, **8**(3), 199-249.